Institut EURECOM
2229, route des Crêtes
B.P. 193
06904 Sophia Antipolis
FRANCE

Research Report N° 94-017

Edge Detection
on Ultrasound Cardiac Images
using Mathematical Morphology
and Active Contours

Jean-Pierre Guy   Jean-Luc Dugelay

November 25, 1994

Telephone:	+33 93 00 26 26	E-mail:
Jean-Luc Dugelay:	+33 93 00 26 41	dugelay@eurecom.fr
Fax:	+33 93 00 26 27	

Edge Detection on Ultrasound Cardiac Images using Mathematical Morphology and Active Contours

J.-P. Guy, J.-L. Dugelay

Institut EURECOM, Mutimedia Communications Dpt.
2229, route des Crêtes, B.P. 193, F-06904 Sophia Antipolis Cedex
correspondance e-mail: dugelay@eurecom.fr

Summary

For an accurate diagnosis of cardiac myopathy, information about heart muscle contractibility is essential. It can be extracted from an ultrasound 2D image by computing the boundaries of ventricle areas. The goal of this study is to find a suitable algorithm yielding a closed curve which tracks ventricle boundaries even for the difficult-to-scan patient where the image is very noisy. Simulations show that using mathematical morphology and active contours allow detection and tracking of edges to help make medical diagnosis.

Keywords: cardiac imaging, help diagnosis, pathology detection, edges, mathematical morphology, active contours.

Résumé

Pour diagnostiquer une pathologie telle que la myopathie, il est nécessaire d'étudier les contractions du muscle cardiaque. Cela peut se faire en détectant les contours sur des images acquises par un scanner à ultrasons. Le but de cette étude est de développer un algorithme permettant de détecter et de suivre l'évolution des ventricules, et ce même si les séquences sont bruitées. Les résultats obtenus en simulation montrent que l'utilisation de la morphologie mathématique et des contours actifs permet une détection et un suivi temporel des contours suffisants pour une aide au diagnostic médical.

Mots-clés: imagerie cardiaque, aide au diagnostic, détection d'une pathologie, contours, contours actifs, morphologie mathématique.

1

I. Introduction

In this paper, we present an algorithm able to detect ventricles in ultrasound images [1] and to track them along a cardiac cycle. The complete algorithm is composed of three steps (figure n°1): noise reduction, edge dectection, edge closing and tracking (section 2, 3 and 4). Section 2 deals with noise reduction in ultrasound images. Two kinds of noise are considered here: still reflexion located on the right ventricle, and speckle. This is achieved by lowpass filtering. Section 3 shows how left and right ventricle edges are detected by morphology operations, such as erosion and dilatation, applied on the gradient maps. Edge closing and tracking are shown in section 4 to rely on a discrete active contour method. Preliminary results obtained on simulations are presented in each section of this paper. In order to allow for a realizable implementation, we restrict our research to algorithms with low complexity. In the last section, we discuss a possible future hardware implementation of the proposed scheme, as well as techniques for automatic diagnosis.
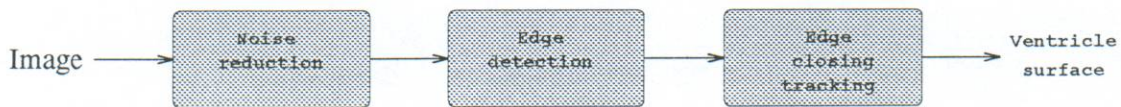

figure n°1

II. Noise reduction

Scanning by ultrasound has the avantage of a non-invasive approach, and its cost is relatively low in comparison with other technics as RMN. However, images obtained have a low contrast and are not directly usable for image processing because of noise.

Observation of ultrasound cardiac images shows that two kinds of noise could interfere with edge dectection: still reflexion (on the right ventricle) and speckle [2].
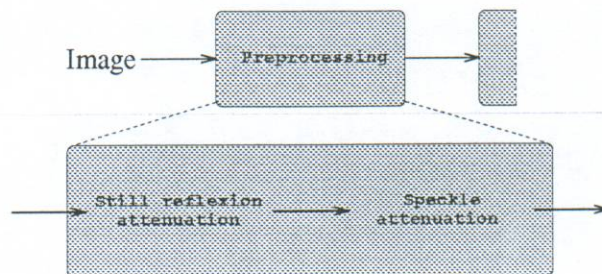

figure n°2

2

Pixels corresponding to a still reflexion area can be detected by temporal observation. These pixels are characterized on the one hand, by a high temporal mean intensity, and, on the other hand, by a low temporal variance intensity. Still reflexion effects are then reduced by applying spatial lowpass filtering on these pixels for each image of the sequence.
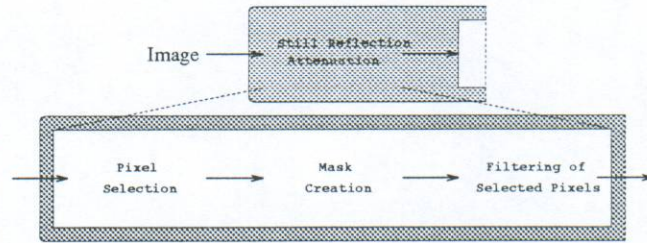

figure n°3

Speckle is present in dark areas of an image which correspond to cavities such as ventricles. Speckle is attenuated by lowpass filtering. A good compromise between noise reduction and significant information conservation can be obtained in two stages [3], as shown in the previous figure and illustrated by images 1, 2 and 3:

- Firstly, low-pass filtering, pixel by pixel, by averaging the intensity in a neighbourhood of size 3x3;
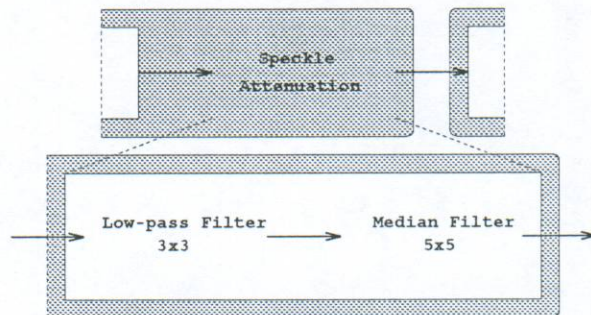- Secondly, median filtering, also pixel by pixel, on a neighbourhood of size 5x5.
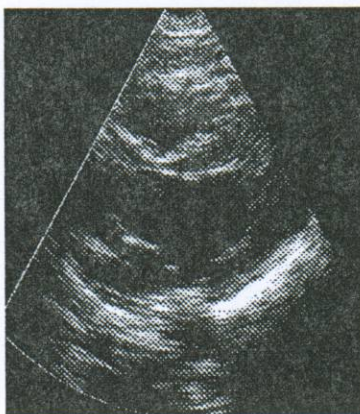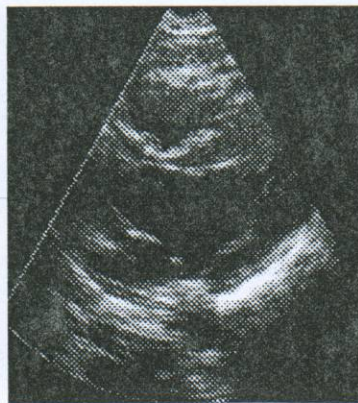

figure n°4

Image n°1
Initial image

Image n°2
Low-pass filtering

Image n°3
Median filtering

3

III. Edge dectection

After still reflexion and speckle attenuation, edge detection is realized in three steps, as shown in the following figure:

Edges detection

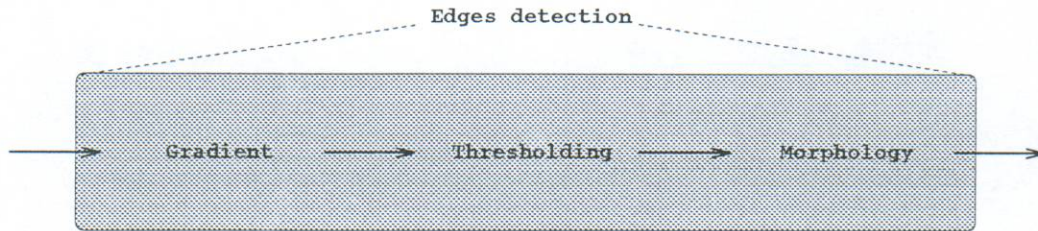Gradient → Thresholding → Morphology

figure n°5

First , we compute the gradient maps by using a classical gradient detector (i.e. Sobel). Then, edge maps are obtained after thresholding and elimination of isolated pixels. Nevertheless, the quality of the maps is not high enough to compute ventricle surfaces and to envisage a temporal tracking of them. Thus, in order to improve edge map quality, we use some basic mathematical morphology transformations on binary images [4], [5], such as erosion and dilation. These operations are realized for a given structuring element, called B_p. For each pixel p of the image, the structuring element is located in such a way that the center of B_p corresponds to p. For a given binary image I, A represents the set of "object" pixels (in white), and (I - A) represents the set of "backgound" pixels (in black).

For the erosion operation, to define the new value of a pixel p, the question is: $B_p \subset A$? For the dilation operation, the question is: $B_p \cap A \neq \varnothing$? If the answer is positive, then p will be considered as an object pixel, otherwise, as a background pixel.

So, the new image C is obtained after performing an erosion or dilation, via a structuring element B_p, and is given by:

$$er(I, B_p) \equiv C = \left\{ p \middle| B_p \subset A \right\}$$

$$dil(I, B_p) \equiv C = \left\{ p \middle| B_p \cap A \neq \varnothing \right\}$$
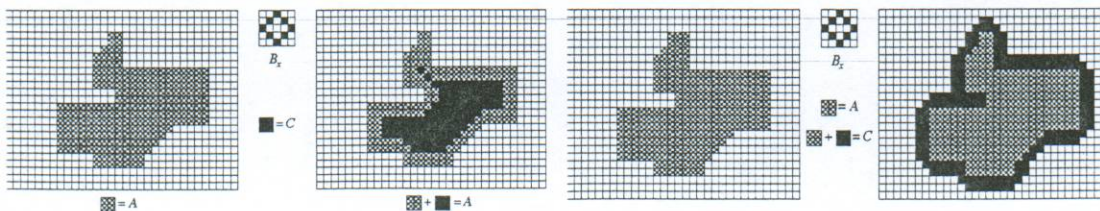

figure n°6 & 7: Illustration of erosion and dilation operations

4

Two other operations can be directly defined from erosion and dilation: opening and closing. Opening is a combination of erosion followed by dilation, realized with the same structuring element: $\mathrm{open}\,(A, B_p) = \mathrm{dil}(\mathrm{er}(I, B_p), B_p)$

Closing is the dual operation, i.e. a combination of dilation followed by erosion, realized with the same structuring element: $\mathrm{close}\,(A, B_p) = \mathrm{er}(\mathrm{dil}(I, B_p), B_p)$

In our case, the best results are obtained by using a closing followed by an opening [3]. The structuring element used here is a discrete circle of diametre 11 pixels for the closing stage (see image 5)) and, also a circle, but of diametre 6, for the opening stage (see image 6). Now ventricle edges may be computed (see image 7).
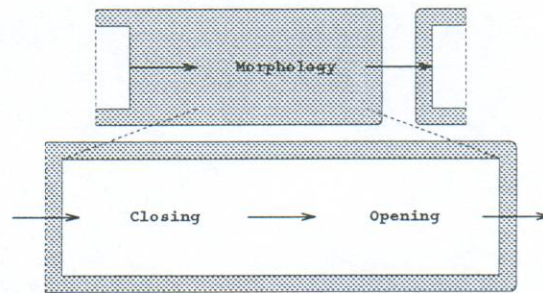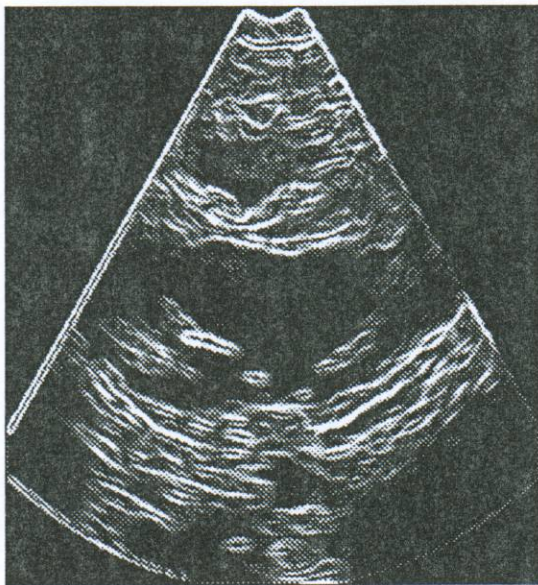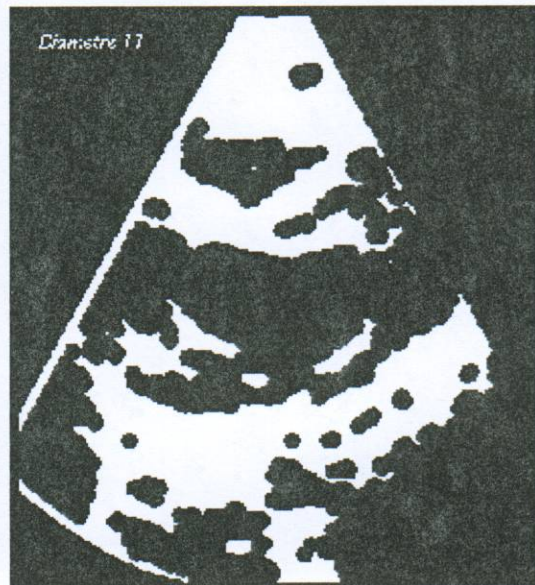

figure n°8

Image n°4: Gradient map

Image n°5: closing
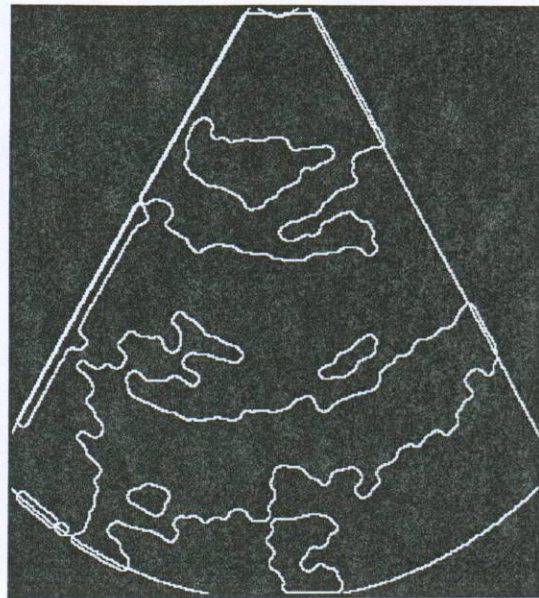
| Image n°6: Opening | Image n°7: Final edge map |

IV. Edge closing and tracking

In order to compute the ventricle surfaces, edges must be closed. This is done by using an elementary discrete active contour model (snake) [6]. More information about snakes can be found in reference [7].
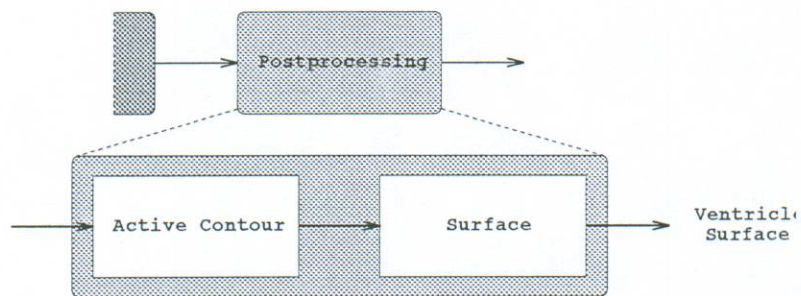

figure n°9

The present application uses deformable contours that have some viscoelasticity and rigidity. We define a discrete deformable contour as a set of n nodes indexed by i=1 ... n. Each node is associated to its time-varying position: $\vec{x}_i(t) = [x_i(t), y_i(t)]^t$ along with tension forces $\vec{\alpha}_i(t)$, rigidity forces $\vec{\beta}_i(t)$, and external forces $\vec{f}_i(t)$.

The nodes are connected in series using nonlinear springs. Following the formulation of [8], the behaviour of the deformable contour is governed by the first order dynamic system:

$$\gamma \frac{d\vec{x}_i}{dt} + \vec{\alpha}_i + \vec{\beta}_i = \vec{f}_i \quad i=1,\dots,n$$

6

where γ a damping coefficient.

The deformable contour is responsive to an image force field that influences its shape and motion. A distance image is first calculated from the edge map, as shown image n°8, which defines a potential function $P(x, y, T)$, in frame T. The force field is expressed as the gradient of this potential function:

$$\vec{f}_i = -\nabla P(\vec{x}_i) \text{ where } \nabla = \left[\frac{\partial}{\partial x}, \frac{\partial}{\partial y} \right]$$
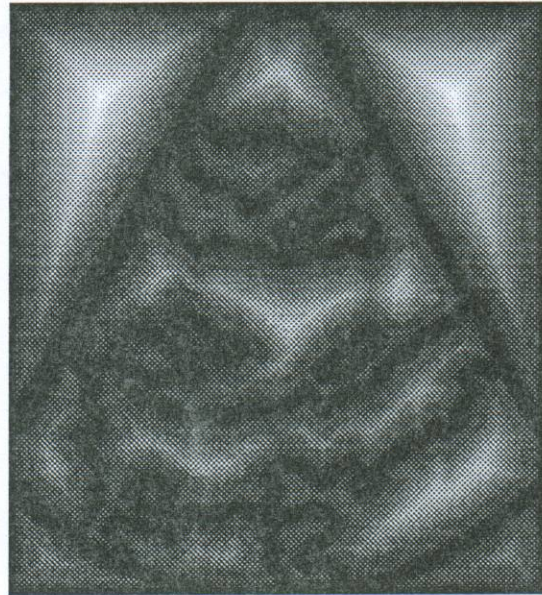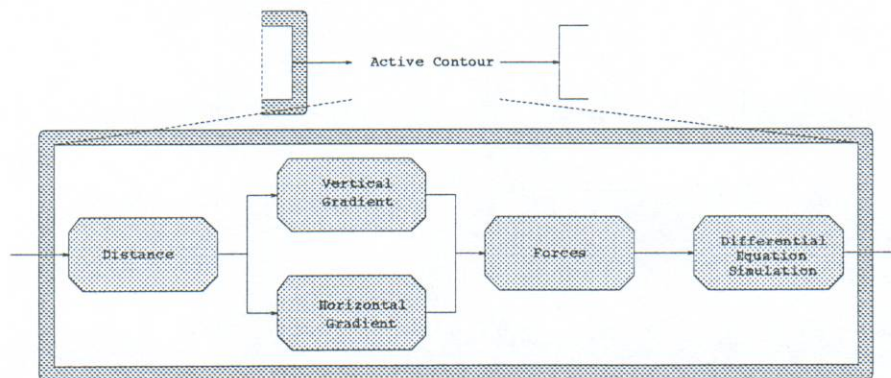

Image n°8

figure n°10

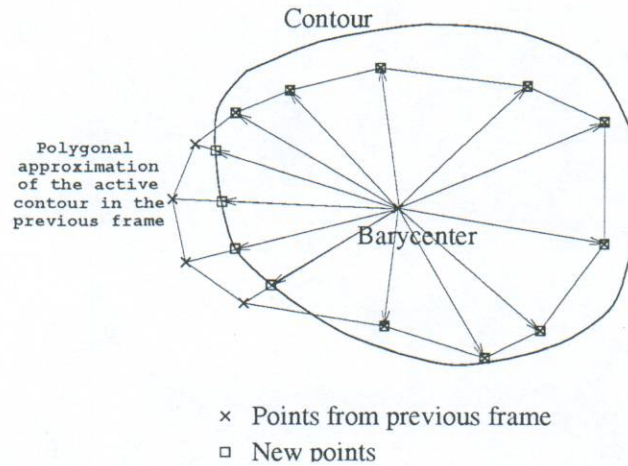In a few simulations steps, the deformable contour slides downhill in $P(x, y, T)$ conforming to the shapes of its ravines. As soon as the contours have converged in $P(x, y, T)$, we replace it with $P(x, y, T+1)$ associated with the next video frame. We repeat the process on successive frames (see figure 11). For the first picture of the sequence, the initialization stage must be done by the medical expert.

figure n°11:

Contour

Polygonal
approximation
of the active
contour in the
previous frame

Barycenter

× Points from previous frame
□ New points

This simple tracking scheme works better if we introduce a varying number of nodes in
the deformable contour. After each simulation step of the differential equation the contour
is resampled: nodes too close are deleted and intermediates nodes are introduced between
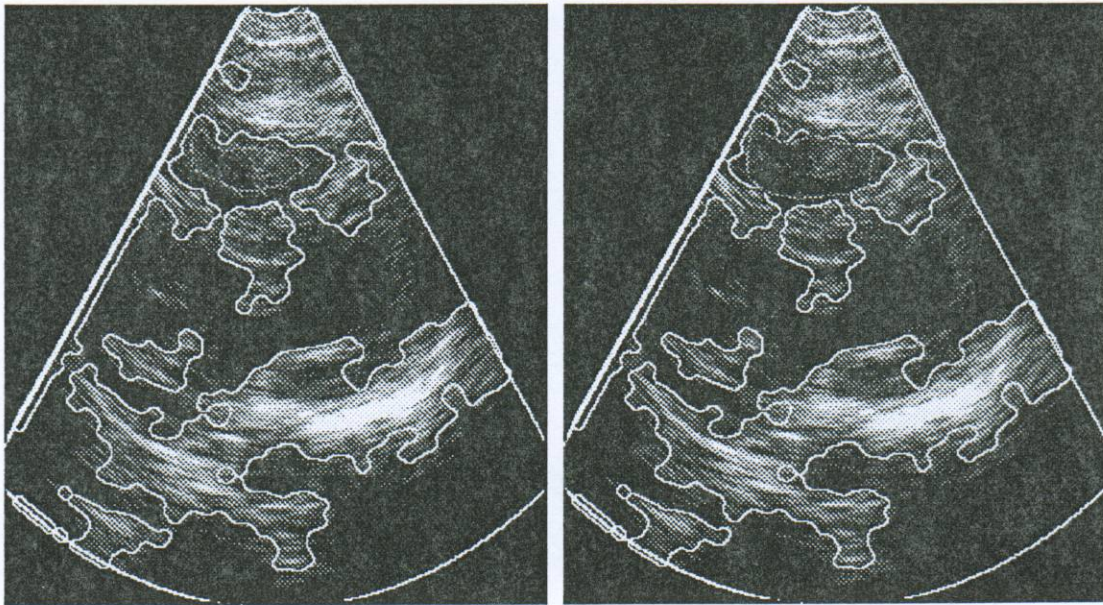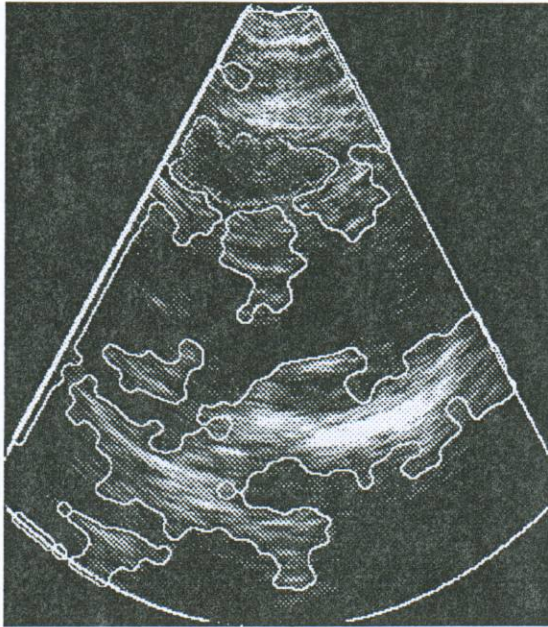two adjacent nodes (Images 9, 10 & 11 show the process for the right ventricle).

Image n°9: Inital step

Image n°10: Intermediate step

Drawing of the active edge is achieved by linear interpolation between nodes. A more accurate spline interpolation may be used [9]. In this case the spline parameters are approximated between two successive nodes using a least square approach.

Image n°11: Final step

As the deformable contour evolves, its dynamic state variables $\vec{x}_i(t)$ provide explicit information for calculating the surface of the ventricles. The surface is then simply computed as shown in figure 12 by the expression:

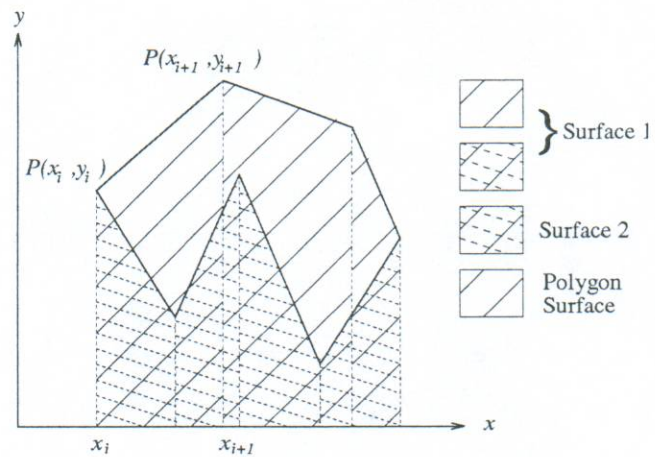$$Surface = \sum_i \left| (x_{i+1} - x_i) \frac{y_{i+1} + y_i}{2} \right|$$

figure n°12

V. Discussion

Simulations are mainly conducted under the Khoros software environment [10]. Currently, besides the choice of the threshold required for the computation of the initial edge map (see section 3 and image n°4), all elements of image processing steps are entirely automatic. Although, the threshold does not vary very much from sequence to sequence, it is not possible to keep it unchanged because of the algorithm's sensitivity to this value. Future work should be devoted on how to compute it as a function of the sequence statistics. Another possibility consists in accepting a manual control as used in gain contrast tuning for instance.

In order to allow a realizable hardware implementation [11], we tried to keep a low algorithmic complexity: Noise reduction requires simple operations as convolution for lowpass filtering and a quick sort for median filtering. Edge detection requires also simple operations like convolution for gradient map computing, and set-operations (an opening and a closing) on the gradient maps to improve it. All these operations could be applied independently on each pixel of the picture. The main difficulty, in an hardware implementation, lies in the last step which uses active edges. This step should be defined more precisely and perhaps simplified.

The current algorithm gives information in terms of ventricle surface variations to the medical expert in order to help him determine a pathology. A supplementary step could consist in suggesting a diagnostic, based on information extracted by the algorithm, namely as ventricle surface variations, and using a priori information given by a medical expert about some pathology features.

10

References

[1] I.L. Herblin and N. Ayache, "Features Extraction and Analysis Methods for Sequences of Ultrasound Images", Image and Vision Computing, Vol. 10, No. 10, December 1992.

[2] J. M. Thijssen, B.J. Oosterveld, "Texture in Tissue Echograms: Speckle or Information?", J. Ultrasound Med. 9:215-229, 1990.

[3] J.-P. Guy, "Détection de Contours sur Echographies Cardiaques", Training Report, Juillet 94. Eurecom, http://www.cica.fr

[4] J. Serra, "Introduction to Mathematical Morphology", Computer Vision, Graphics and Image processing, 1986, Vol. 35, pp. 283-305.

[5] N. Rougon & F. Prêtreux, "Deformable Markers: Segmentation using active contours and mathematical morphology", 8ième Congrés AFCET-RFIA, Lyon Villeurbanne, 25-29 novembre 91.

[6] D. Terzopoulos and K. Waters, "Analysis and Synthesis of Facial Image Sequences", IEEE Trans. on PAMI, June 1993, Vol. 15, no. 6, pp. 569-579.

[7] I. Cohen, "Modèles Déformables 2-D et 3-D: Application à la segmentation d'Images Médicales", Thèse de doctorat de l'Université Paris IX, 1992.

[8] M. Kass, A. Witkin, and D. Terzopoulos, "Snakes: Active Contours Models", International Journal of Computer Vision, 1988, pp. 321-331.

[9] D.H. Kochanek and R. H. Bartels, "Interpolating Splines with Local Tension, Continuity, and Bias Control", ACM, Computer Graphics, Vol. 18, No. 3, pp.33-41, July 1984.

[10] K. Konstantinides and J.R. Rasure, "The Khoros Software Development Environment for Image and Signal Processing", IEEE Trans. on Image Processing, Vol. 3, No. 3, May 1994.

[11] H.E. Melton, Jr and D.J. Skorton, "Real-time automatic Boundary Detection in Echocardiography", 1992 Ultrasonics Symposium.